# Continuous-wave diode-pumped laser action of $Nd^{3+}$-doped photo-thermo-refractive glass

**Yoichi Sato,[1,*] Takunori Taira,[1] Vadim Smirnov,[2] Larissa Glebova,[2] and Leonid Glebov[3]**

[1]*Laser Research Center for Molecular Science, Institute for Molecular Science, 38 Nishigonaka, Myodaiji, Okazaki 444-8585, Japan*

[2]*OptiGrate, Inc., 3267 Progress Drive, Orlando, Florida 32826, USA*

[3]*CREOL/The College of Optics and Photonics, University of Central Florida, 4000 Central Florida Boulevard, Orlando, Florida 32816-2700, USA*

**Corresponding author: yoichi@ims.ac.jp*

Received March 21, 2011; revised May 16, 2011; accepted May 16, 2011; posted May 16, 2011 (Doc. ID 144445); published June 8, 2011

Laser action of the photo-thermo-refractive (PTR) glass, which is the photosensitive material for holographic recording of volume Bragg gratings (VBGs), was demonstrated for the first time by introducing $Nd^{3+}$. Nd:PTR glass has a bandwidth of 27.8 nm and 16.0 nm for luminescence and absorption, respectively. An uncoated 2 mm thick Nd:PTR element generated cw laser output of 124 mW, with a slope efficiency of 25%, by laser diode pumping. This Nd:PTR glass also performed wide bandwidth laser action at 1053.9–1063.3 nm, where the decrease of the pump-absorption efficiency was held off below 30%, even under a 3.5 nm shift of pump wavelength from its absorption center. 

*OCIS codes:* 140.3380, 140.3480, 140.5680.

In recent years various novel optical functions have been achieved by the progress of *micro solid-state photonics*, which is based on microdomain control technologies for optical materials such as polycrystalline laser ceramics [1], periodically poled ferroelectric quasi-phase matching devices [2], and volume Bragg grating (VBG) [3]. VBGs especially have been demonstrating various novel functions: wavelength stabilization [4], ultrashort pulse stretching and compressing [5], spectral beam combination [6], narrowband filters [7], angular beam deflection [8], and so on.

It is very effective for evolving micro solid-state photonics to integrate the VBG device and the laser active medium. VBGs are made of the photo-thermo-refractive (PTR) glass that has photosensitivity and the composition of $15Na_2O$-$5ZnO$-$5Al_2O_3$-$75SiO_2$ doped with Ag, Ce, F, and Br [9]. It was already proven that codoping of PTR glass with a second rare-earth component does not eliminate its photosensitivity for making Bragg gratings [3]. The study of rare-earth-doped PTR glass for the laser host material is very interesting and attractive because it enables laser active media to perform all optical functions realized by VBG technologies.

In this Letter we performed a laser oscillation of $Nd^{3+}$-doped PTR (Nd:PTR) glass under laser diode pumping and discussed advantages of Nd:PTR glass as a laser medium for future VBG laser oscillators. To our knowledge, this is the first report of a laser oscillation with photosensitive athermal glass, which promises VBG laser media that perform alignment-free, single-longitudinal single-mode wavelength-tunable lasing. It is another concept of a microchip laser [10].

The Nd:PTR glass sample was fabricated as it was described in the United States patent [9]. The sample prepared for this research was codoped with 0.8 at.% of $Nd^{3+}$. This sample was slab shaped with a thickness of 1.93 mm, and its large surface with dimensions of 25.0 mm × 24.0 mm was polished. In the following research, no additional coating layer was done on the sample surfaces.

The measurement of absorption spectrum was carried out by using a spectrophotometer (U-3500, Hitachi) with at most 0.2 nm resolution. During the fluorescence spectrum measurement, this sample was excited by 808 nm radiation of an optical parametric oscillation with pulses of 3 ns duration (MOPO-HF, Spectra-Physics) pumped by a third harmonic Nd:YAG laser (PRO-250-10, Spectra-Physics). Emitted photons from the excited sample were analyzed by a monochromator (TRIAX-550, JOBIN YVON) with up to 0.15 nm resolution and detected by a linear-InGaAs-array detector (IGA512-1 × 1, JOBIN YVON). A Czochralski-grown 1.0 at.% Nd:YAG single crystal (Scientific Materials Co.) was used in order to compare the fluorescence spectra.

Laser performance of the Nd:PTR glass sample was examined by using of a plane-concave cavity of 50 mm length. This cavity had an output coupler with 100 mm curvature radius and a flat rear dichroic mirror with high reflection around 1064 nm and high transmission at 808 nm. The Nd:PTR glass was sandwiched by the copper plates, and it was placed inside the cavity 5 mm away from the rear mirror. The temperature of this copper plate was maintained at 23 °C by a thermo-electric controller (LDT-5948, ILX Lightwave Co.). After the pump beam from a fiber-coupled 808 nm laser diode with core diameter of 400 $\mu$m and N.A. of 0.22 (LIMO40-F400-DL808, LIMO GmbH) was collimated by a lens of 100 mm focal length, it was focused into the Nd:PTR glass through a high-reflectivity mirror with a lens of 50 mm focal length. Emission spectra of a pump source and laser output extracted from the Nd:PTR glass were measured with an optical spectrum analyzer (Q8384, Advantest). The $M^2$ value of the laser output was evaluated by a laser beam analyzer (Modemaster, Coherent, Inc).

 

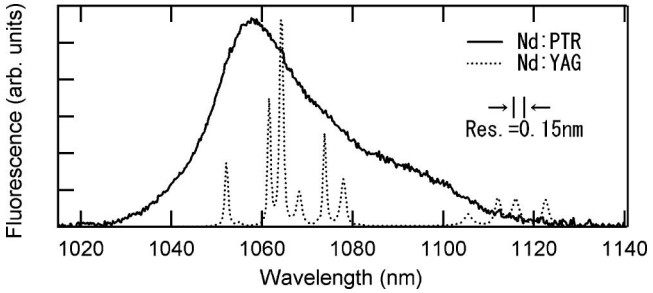


Fig. 1. Fluorescence spectra of Nd:PTR glass (solid curve) and Nd:YAG (dotted curve).

Figure 1 shows a fluorescence spectrum of Nd:PTR glass and Nd:YAG. The center wavelength of fluorescence from the Nd:PTR glass was 1057.7 nm, and its emission bandwidth was 27.8 nm. An absorption coefficient of 0.8 at.% Nd:PTR glass for the $Nd^{3+}$ transition between $^4I_{9/2}$ and $^4F_{3/2}$ was 1.4 $cm^{-1}$ with a bandwidth of 16.0 nm at the absorption center of 806.0 nm. The reflection loss for transmitted light at the sample surfaces was estimated to be 6.9%. The spectral bandwidths of Nd:PTR glass were 25 and 13 times wider than those for the central peak of Nd:YAG for fluorescence and absorption, respectively.

Laser input–output characteristics of the uncoated Nd:PTR glass sample are shown in Fig. 2. A slope efficiency $\eta$ of 24.9% was achieved by use of 3% output coupling mirror. Maximum output power of 124 mW was obtained under 639 mW absorbed power (3 W pumping). The value of the $M^2$ factor of laser output at the maximum output power was 8.

Figure 3 shows the longitudinal mode spectrum of the Nd:PTR laser. The obtained Nd:PTR laser had a multimode output, including modes between 1053.9 and 1063.3 nm.

In the end-pumped microchip laser system, the high $M^2$ value of an output laser beam is mainly caused by the larger spot size $w_P$ of a pump beam focused on the laser medium than the radius $w_L$ of the fundamental transverse laser mode [11]. Since the Nd:PTR glass plate was positioned near the beam waist of the plano-concave resonator in our study, $w_L$ was estimated to be 370 $\mu$m. In order to reduce the $M^2$ factor that corresponds to a single transverse mode, $w_L$ should be decreased to 130 $\mu$m and $w_P$ must be less than 130 $\mu$m. Although $w_P$ on the front surface of the gain element was 100 $\mu$m, $w_P$ on the rear surface increased to 482 $\mu$m. This is the reason why an

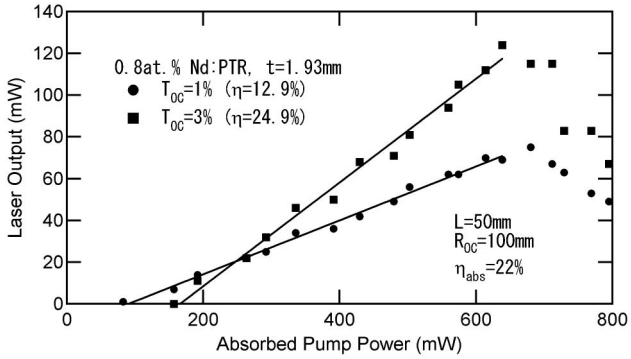


Fig. 2. Laser performance of 0.8 at.% Nd:PTR glass with output coupling of 1% and 3%.

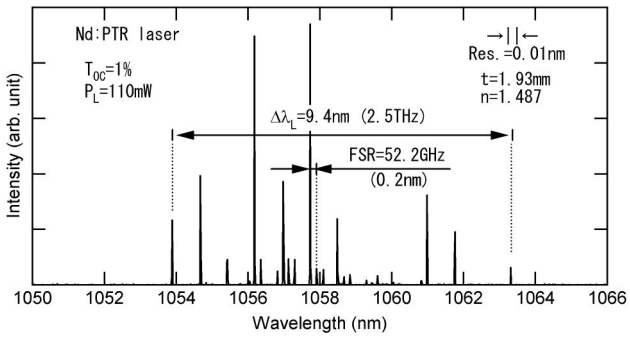


Fig. 3. Longitudinal mode of Nd:PTR laser output.

effective $w_P$ in the laser medium in the studied setup became 370 $\mu$m that caused a multimode regime with an $M^2$ factor of 8.

The obtained $\eta$ of 24.9% was much smaller than the theoretical limit calculated from atomic quantum efficiency $\eta_{qd}$, which is the ratio of photon energy between pump source and laser output. The reduction of $\eta$ is caused by the round-trip loss of the resonator $L$ and the mode-matching efficiency between the pump beam and the output beam, $\eta_m$. We can estimate $L$ by changing the output coupling: $L$ is given by [12]

$$L = \frac{\eta_1 - \eta_2}{\eta_2 T_1 - \eta_1 T_2} T_1 T_2, \tag{1}$$

where $\eta_1$ and $\eta_2$ are the slope efficiencies when the output couplers of $T_1$ and $T_2$ are used in a laser cavity. From Fig. 2 and Eq. (1), $L$ is calculated to be 2.6%, which is considered to be mainly due to the Fresnel loss of the uncoated Nd:PTR glass plate. Here we can calculate $\eta_m$ to be 61.2% as an effective value by

$$\eta_i = \frac{T_i}{T_i + L} \eta_m \eta_{qd}, \tag{2}$$

where $\eta_m$ corresponds to the ratio of the mode volume inside the laser active media between the pump source and the output beam mode.

Thus, by only having antireflection coating ($L \sim 0.2\%$) on the surface of the Nd:PTR glass, $\eta$ should be improved to 43.6%. For further improvement of $\eta$, it is required to increase $\eta_m$ by modifying the cavity condition. When the beam waist $w_0$ becomes larger than $w_P$ inside the Nd:PTR glass, both $\eta_m$ and the $M^2$ factor should approach 1. This condition will be satisfied by adjusting the curvature of output coupler $R$ to 700 mm or more with a semiconfocal cavity condition. In order to keep 50 mm of the cavity length, $R$ should be larger than 10,000 mm.

The most important point in the development of rare-earth-doped solid-state laser media is to prevent the quenching of luminescence by clustering of $Nd^{3+}$ [13]. This quenching effect causes the reduction of the product of the stimulated emission cross section and fluorescence lifetime $\sigma\tau$. Thus, by comparing $\sigma\tau$ of Nd:PTR glass with traditional multicomponent silicate glasses, e.g., ED-2 [14], we can judge whether our Nd:PTR glass was developed successfully or not. $\sigma\tau$ can be estimated from a threshold power $P_{\text{th}}$ by

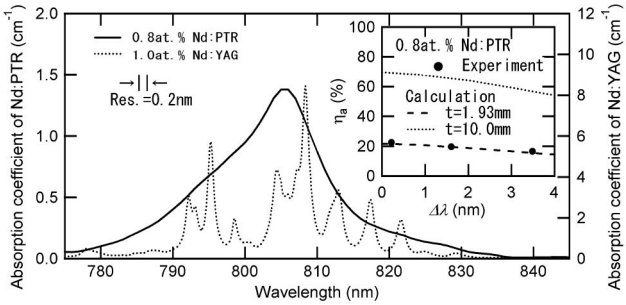


Fig. 4. Absorption coefficients of 0.8 at.% Nd:PTR glass and 1.0 at.% Nd:YAG (solid and dotted curves, respectively). $\eta_a$ of the Nd:PTR laser is also shown in inset, where experimental value (circles) coincides with the calculation (dashed and dotted curves).

$$P_{\mathrm{th}} = \frac{h\nu_p}{2\sigma\tau} A(T+L), \tag{3}$$

where $h$, $\nu_p$, $A$, and $T$ are Plank's constant, the frequency of the pump beam, the cross section of the laser mode volume, and the output coupling, respectively. In Fig. 2 $P_{\mathrm{th}}$ is 157 mW with $T$ of 3%. Since the threshold of laser oscillation in an end-pumped solid-state laser has a single transverse fundamental mode, $\sigma\tau$ is calculated to be $2324\,\mathrm{pm}^2 \cdot \mu\mathrm{s}$. This $\sigma\tau$ is 1.7 times larger than ED-2 [14], which suggests that we can avoid $Nd^{3+}$ clustering in Nd:PTR glass by introducing photosensitivity. Therefore, Nd:PTR glass is expected to be one of the best candidates for the laser medium among $Nd^{3+}$-doped glasses.

We observed a sharp drop of output power with the increase of the pump as shown in Fig. 2, which was generally considered to be due to a thermal-lensing effect. Although the athermal nature of PTR glass can avoid the influence caused by the change of optical path length, temperature distribution on the surface of Nd:PTR glass induced by the laser diode pumping causes nonuniform stress in the gain volume. Therefore, stress-induced lensing and birefringence should be the origin of this fast drop of laser output. Also, other origins like thermal quenching of luminescence or the upconversion process might reduce the laser efficiency. Further discussions are necessary to evaluate more detailed spectroscopic characteristics of Nd:PTR glass.

The spectral bandwidth of the Nd:PTR laser output in this study was 9.4 nm. The calculated longitudinal mode spacing was 52.2 GHz (0.2 nm), which was appropriate for a free spectrum range of Fabry–Perot resonator produced by uncoated surfaces of the PTR glass plate with 1.93 mm thickness. Potentially, 28 nm bandwidth in an Nd:PTR laser can be realized from the viewpoint of a bandwidth of the fluorescent spectrum. This wide bandwidth is quite useful for micro solid-state photonics: for example, wavelength tunability and controllability of laser output from Nd:PTR glass as the gain medium with a VBG structure, ultrashort mode-locked pulse generation of 42 fs Fourier transform limit, etc.

We should make a special mention of the broad absorption bandwidth advantage of Nd:PTR shown in Fig. 4. Because the temperature of the laser diode pump was not controlled under this evaluation, the wavelength of emitted power from the laser diode varied from 805 to 810 nm under the laser experiments. Figure 4 also shows the coincidence of pump-absorption efficiency, $\eta_a$ between the experimentally performed value and the calculated value from the absorption coefficient of Nd:PTR glass. Although the wavelength shift of the pump source from absorption center, $\Delta\lambda$, reached 3.5 nm from the absorption center of 806 nm, the degradation of pump-absorption efficiency was limited to be only 30%. It is demonstrated in Fig. 4 that a thicker absorption length reduces this degradation in pump-absorption efficiency.

In conclusion, we have demonstrated the laser oscillation of $Nd^{3+}$-doped PTR glass for the first time. The resulting laser performance proves the significance of Nd:PTR laser media, which have wide absorption and emission spectra. Thanks to a wide absorption bandwidth in Nd:PTR glass, this laser is almost free from a degradation of laser performance due to temperature-induced emitting wavelength variation of a pump laser diode unit. The wide emission bandwidth will enable broadly tunable single-mode laser oscillations by using of a VBG-structured Nd:PTR laser medium. Rare-earth-doped PTR glass will provide novel functional devices based on VBG technologies, which should find wide applications in micro solid-state photonics.

The authors acknowledge Dr. Rakesh Bahndari for helpful comments on the manuscript. This work was partially supported by the Genesis Research Institute, Inc., Nagoya, Japan, and National Aeronautics and Space Administration (NASA), USA.

**References**

1. T. Taira, IEEE J. Sel. Top. Quantum Electron. **13**, 798 (2007).
2. H. Ishizuki, I. Shoji, and T. Taira, Appl. Phys. Lett. **82**, 4062 (2003).
3. L. Glebov, Proc. SPIE **6216**, 621601 (2006).
4. N. Vorobiev, L. Glebov, and V. Smirnov, Opt. Express **16**, 9199 (2008).
5. K.-H. Liao, M.-Y. Cheng, E. Flecher, V. I. Smirnov, L. Glebov, and A. Galvanauskas, Opt. Express **15**, 4876 (2007).
6. O. Andrusyak, V. Smirnov, G. Venus, V. Rotar, and L. Glebov, IEEE J. Sel. Top. Quantum Electron. **15**, 344 (2009).
7. J. Lumeau, L. Glebov, and V. Smirnov, Opt. Lett. **31**, 2417 (2006).
8. A. L. Glebov, V. I. Smirnov, M. G. Lee, L. B. Glebov, A. Sugama, S. Aoki, and V. Rotar, IEEE Photon. Technol. Lett. **19**, 701 (2007).
9. O. Efimov, L. Glebov, V. Smirnov, and L. Glebova, "Process for production of high efficiency volume diffractive elements in photo-thermo-refractive glass," U.S. patent 6,586,141 (July 1, 2003).
10. T. Taira, A. Mukai, Y. Nozawa, and T. Kobayashi, Opt. Lett. **16**, 1955 (1991).
11. T. Taira, N. Pavel, M. Furuhata, M. Ohtaka, and K. Kobayashi, in *Advanced Solid State Lasers*, W. Bosenberg and M. Fejer, eds., Vol. 19 of OSA Trends in Optics and Photonics Series (Optical Society of America, 1998), paper NA9.
12. I. Shoji, S. Kurimura, Y. Sato, T. Taira, A. Ikesue, and K. Yoshida, Appl. Phys. Lett. **77**, 939 (2000).
13. Y. Quao, N. Da, D. Chen, W. Ma, Q. Zhou, and J. Qiu, J. Mater. Sci. **44**, 4026 (2009).
14. M. Birnbaum and J. A. Gelbwachs, J. Appl. Phys. **43**, 2335 (1972).